

# New approach to the theory of intermediate valence.

## II. Magnetic susceptibility and magnetic instabilities

M. E. Foglio

*Instituto de Fisica "G. Wataghin", Universidade Estadual de Campinas, 13100 Campinas, S. P., Brazil*

C. A. Balseiro\* and L. M. Falicov

*Department of Physics, University of California, Berkeley, California 94720*

(Received 5 March 1979)

The previously introduced formalism to study the properties of some intermediate-valence solids is applied to calculate the magnetic susceptibility of various models and the instabilities of the paramagnetic state against ferromagnetism and antiferromagnetism. Our main results are: (i) A considerably enhanced susceptibility consisting of (a) a Hubbard-type Pauli contribution and (b) a Van-Vleck-type term due to higher configuration admixing. (ii) Instabilities against ferromagnetism and antiferromagnetism which are independent of the Van Vleck-type contribution and which differ somewhat from similar divergences found in the Hubbard model.

### I. INTRODUCTION

In the preceding paper<sup>1</sup> (hereafter referred to as I) a theory of intermediate valence was presented. The original Hamiltonian consisted of three terms:

(i) A band term in a magnetic field

$$\mathcal{H}_b = \sum_{\langle ij \rangle \sigma} t c_{i\sigma}^\dagger c_{j\sigma} + \sum_i h (c_{i\uparrow}^\dagger c_{i\uparrow} - c_{i\downarrow}^\dagger c_{i\downarrow}) \quad (1.1)$$

where  $c_{i\sigma}^\dagger$  and  $c_{i\sigma}$  are the creation and destruction operators for Wannier states at site  $i$  and spin  $\sigma$ ,  $t$  is a band hopping parameter between nearest-neighbor sites  $\langle ij \rangle$ , and  $h$  is the externally applied magnetic field multiplied by  $\frac{1}{2}(g_e \mu_B)$ .

(ii) An ionic contribution which measures the energy of a ground configuration  $(4f)^n$  as zero and the states  $M$  of an excited configuration  $(4f)^{n+1}$  as  $E_M$

$$\mathcal{H}_i = \sum_{JM} E_M B_{JM}^\dagger B_{JM} \quad (1.2)$$

we have taken the ground configuration to be a singlet  $|G\rangle$  and the configuration  $(4f)^{n+1}$  to be a doublet  $|+\rangle, |-\rangle$ . The modified Fermi operators,  $B_{JM}^\dagger, B_{JM}$  defined elsewhere,<sup>2</sup> satisfy  $B_{JM}^\dagger B_{JM'}^\dagger = 0$ , which guarantees no simultaneous occupation of  $|+\rangle$  and  $|-\rangle$ . The energies of the excited states in the  $(4f)^{n+1}$  configuration are

$$E_\pm = E \pm g_0 h \quad (1.3)$$

where  $g_0$  is the ratio of the ionic to the conduction electron  $g$  factors.

(iii) A hybridization term,

$$\mathcal{H}_h = \sum_{JM\sigma} V_{M\sigma} (B_{JM}^\dagger c_{J\sigma} + c_{J\sigma}^\dagger B_{JM}) \quad (1.4)$$

where

$$V_{+1} = V_{-1} = V, \quad V_{+1} = V_{-1} = 0 \quad (1.5)$$

Our method consists of (a) complete diagonalization of the intra-atomic terms (1.2), (1.4), and the second term in (1.1); (b) projecting out of the upper eight ionic states, retaining only the lowest four for each ion; (c) conversion of these four states into equivalent spin- $\frac{1}{2}$  fermion states  $|0\rangle, |\uparrow\rangle, |\downarrow\rangle$ , and  $|\uparrow\downarrow\rangle$  and definition of their corresponding fermion creation ( $\gamma_{i\sigma}^\dagger$ ) and destruction ( $\gamma_{i\sigma}$ ) operators; (d) expression of all the terms, the band terms in (1.1) in particular, in terms of these new operators; and (e) treatment of the resulting Hamiltonian, which includes one-particle ( $\gamma^\dagger \gamma$ ), two-particle ( $\gamma^\dagger \gamma \gamma^\dagger \gamma$ ), and three-particle ( $\gamma^\dagger \gamma \gamma^\dagger \gamma \gamma^\dagger \gamma$ ) terms by a decoupling scheme analogous to the Hartree-Fock approximation.

The resulting Hartree-Fock Hamiltonian is

$$H_{\text{HF}} = \sum_{J\sigma} U_{J\sigma} \gamma_{J\sigma}^\dagger \gamma_{J\sigma} - \sum_{\langle ij \rangle \sigma} W_{ij\sigma} \gamma_{i\sigma}^\dagger \gamma_{j\sigma} + K \quad (1.6)$$

where the  $c$ -numbers  $U_\sigma$ ,  $W_\sigma$ , and  $K$  depend self-consistently on expectation values of the form  $\langle \gamma_{i\sigma}^\dagger \gamma_{i\sigma} \rangle$  and  $\langle \gamma_{i\sigma}^\dagger \gamma_{j\sigma} \rangle$ , as well as on the coefficients ( $\alpha$ 's,  $\beta$ 's, and  $\delta$ 's) which appear in the diagonalization of the ionic states

$$\begin{aligned} |0\rangle &\equiv |G0\rangle, \\ |\uparrow\rangle &\equiv \alpha_u |G\uparrow\rangle + \beta_u |+\rangle; \\ |\downarrow\rangle &\equiv \alpha_d |G\downarrow\rangle + \beta_d |-\rangle; \\ |\uparrow\downarrow\rangle &\equiv \alpha_s |G\uparrow\downarrow\rangle + \delta_u |+\rangle + \delta_d |-\rangle. \end{aligned} \quad (1.7)$$

The energies of these states are  $E_0=0$ ;  $E_\uparrow, E_\downarrow$ , and  $E_{\uparrow\downarrow}$ .

In this paper we apply this formalism to study the magnetic susceptibility of the paramagnetic state. We apply this calculation to well-defined structures as a function of the dynamic parameters  $t$ ,  $E$ ,  $V$ , and  $g_0$ .

as well as of the average number of electrons per ion  $(n + \nu)$ , where  $n$  is the number of electrons in the  $(4f)^n$  configuration and  $0 \leq \nu \leq 2$ . In Sec. II we describe the method employed to calculate the self-consistent expectation values. In Sec. III we calculate the uniform magnetic susceptibility of several models and determine the instability conditions against ferromagnetism. Section IV deals with the  $\bar{Q} \neq 0$  susceptibilities for specific examples and the instabilities against antiferromagnetism. Section V contains a summary and conclusions.

## II. CALCULATION OF SELF-CONSISTENT AVERAGES FOR THE PARAMAGNETIC AND FERROMAGNETIC STATES

For states with complete translational symmetry, i.e., the paramagnetic and ferromagnetic states, a change from localized operators,  $\gamma_{j\sigma}^\dagger$  and  $\gamma_{j\sigma}$  to Bloch state operators  $\Gamma_{k\sigma}^\dagger$  and  $\Gamma_{k\sigma}$

$$\Gamma_{k\sigma} \equiv (N)^{-1/2} \sum_j \exp(i\vec{k} \cdot \vec{R}_j) \gamma_{j\sigma} \quad (2.1)$$

automatically reduces Eq. (1.6) to diagonal form

$$H_{\text{HF}} = \sum_{k\sigma} E_{k\sigma} \Gamma_{k\sigma}^\dagger \Gamma_{k\sigma} + K, \quad (2.2)$$

where, for  $W_\sigma > 0$ ,

$$E_{k\sigma} \equiv U_\sigma + W_\sigma S(\vec{k}) \quad (2.3)$$

and

$$S(\vec{k}) \equiv - \sum_{\delta, \text{nn}} \exp(i\vec{k} \cdot \vec{R}_\delta), \quad (2.4)$$

with nn being nearest neighbors. The function  $S(\vec{k})$  is a dimensionless band structure with a well-defined lower bound  $S_m$  [e.g.,  $(-6)$  for simple cubic,  $(-8)$  for body-centered, and  $(-12)$  for face-centered cubic] as well as an upper bound  $S_M$   $[(+6)$  for sc;  $(+8)$  for bcc, and  $(+4)$  for fcc].

We now define two "Fermi levels"  $S_\sigma$  such that for spin  $\sigma$ , states with  $S(\vec{k}) \leq S_\sigma$  are occupied and those with  $S(\vec{k}) > S_\sigma$  are empty. We also define  $f_\sigma(\vec{k})$  such that

$$f_\sigma(\vec{k}) = \begin{cases} 1, & S(\vec{k}) \leq S_\sigma \\ 0, & S(\vec{k}) > S_\sigma \end{cases} \quad (2.5)$$

With these definitions we may now introduce the basic functions which are necessary for the calculation of the self-consistent averages. These are

$$\rho_\sigma = \rho(S_\sigma) \equiv N^{-1} \sum_k f_\sigma(\vec{k}) \quad (2.6)$$

and

$$\tau_\sigma = \tau(S_\sigma) \equiv N^{-1} \sum_k \exp(i\vec{k} \cdot \vec{R}_\delta) f_\sigma(\vec{k}). \quad (2.7)$$

In Eq. (2.7)  $\vec{R}_\delta$  is a nearest-neighbor lattice vector; it can be proved that for the states under consideration  $\tau_\sigma$  is not a function of the particular  $\vec{R}_\delta$  chosen as long as all  $\vec{R}_\delta$  are symmetry related.

It is now easy to prove that for the paramagnetic and ferromagnetic ground states

$$\langle \gamma_{i\sigma}^\dagger \gamma_{i\sigma'} \rangle = \rho_\sigma \delta_{\sigma\sigma'} \quad (2.8a)$$

and

$$\langle \gamma_{i+\delta, \sigma}^\dagger \gamma_{i\sigma'} \rangle = \tau_\sigma \delta_{\sigma\sigma'}. \quad (2.8b)$$

The functions  $\rho_\sigma$  and  $\tau_\sigma$  satisfy several useful properties. In particular

$$\rho_\uparrow + \rho_\downarrow = \nu. \quad (2.9)$$

In addition if  $\rho_\sigma(S_\sigma)$  is considered a function of  $S_\sigma$ , it is proved in Appendix A that in the model with nearest-neighbor interactions only

$$z \tau(S_\sigma) = - \int_{S_m}^{S_\sigma} x \frac{d\rho(x)}{dx} dx, \quad (2.10)$$

where  $z$  is the number of nearest neighbors. If we recall the definitions from I

$$A_\uparrow \equiv (\alpha_u)^2, \quad B_\uparrow \equiv \alpha_u(X_\uparrow - \alpha_u), \quad (2.11)$$

$$D_\uparrow \equiv (X_\uparrow - \alpha_u)^2, \quad X_\uparrow \equiv -(\alpha_d \alpha_s + \beta_d \delta_d),$$

[see Eq. (1.7)] and four equivalent expressions obtained by exchanging  $\uparrow \leftrightarrow \downarrow$  and  $u \leftrightarrow d$ , we now obtain

$$U_\uparrow = E_\uparrow + (E_{\uparrow\downarrow} - E_\uparrow - E_\downarrow) \rho_\downarrow + 2zt(B_\uparrow \tau_\downarrow + D_\uparrow \tau_\downarrow \rho_\downarrow) \quad (2.12)$$

and a similar expression for  $U_\downarrow$ ,

$$W_\uparrow = -t[A_\uparrow + 2B_\uparrow \rho_\downarrow + D_\uparrow(\rho_\downarrow^2 - \tau_\downarrow^2) - 2D_\uparrow \tau_\downarrow \rho_\downarrow] \quad (2.13)$$

and a similar expression for  $W_\downarrow$ , and

$$K = -N[(E_{\uparrow\downarrow} - E_\uparrow - E_\downarrow) \rho_\uparrow \rho_\downarrow + 2zt\{B_\uparrow \rho_\downarrow \tau_\uparrow + B_\downarrow \rho_\uparrow \tau_\downarrow + D_\uparrow \tau_\uparrow(\rho_\downarrow^2 - \tau_\downarrow^2) + D_\downarrow \tau_\downarrow(\rho_\uparrow^2 - \tau_\uparrow^2)\}] \quad (2.14)$$

It should be noted that the limit of well-defined valence corresponds to  $V=0$ , which yields

$$\alpha_u = \alpha_d = \alpha_s = -1, \quad \beta_u = \beta_d = 0,$$

$$\delta_u = \delta_d = 0, \quad E_\uparrow = h, \quad E_\downarrow = -h,$$

$$E_{\uparrow\downarrow} = 0, \quad U_\sigma = E_\sigma, \quad W_\sigma = -t$$

and  $K=0$ . Therefore

$$H_{\text{HF}}(V=0) = \sum_{\langle ij \rangle \sigma} t \gamma_{i\sigma}^\dagger \gamma_{j\sigma} + \sum_i h(\gamma_{i\uparrow}^\dagger \gamma_{i\uparrow} - \gamma_{i\downarrow}^\dagger \gamma_{i\downarrow}), \quad (2.15)$$

which is identical to the original band Hamiltonian (1.1).

The total energy per site of the system can now be written

$$\mathcal{E} = N^{-1} \langle H_{\text{HF}} \rangle = E_1 \rho_1 + E_1 \rho_1 + (E_{11} - E_1 - E_1) \rho_1 \rho_1 \\ + zt [A_1 \tau_1 + A_1 \tau_1 + 2B_1 \rho_1 \tau_1 + 2B_1 \rho_1 \tau_1 + D_1 \tau_1 (\rho_1^2 - \tau_1^2) + D_1 \tau_1 (\rho_1^2 - \tau_1^2)] \quad (2.16)$$

This equation should be minimized with respect to  $\rho_\sigma$  and  $\tau_\sigma$ , subject to the constraints (2.9) and (2.10).

The value at the minimum we denote by  $\mathcal{E}_{\text{eq}}$ .

### III. MAGNETIC SUSCEPTIBILITY

The magnetic susceptibility is obtained from

$$\chi \equiv - \left( \frac{1}{2} g_e \mu_B \right)^2 \left( \frac{\partial^2 \mathcal{E}_{\text{eq}}}{\partial h^2} \right)_{h=0} \quad (3.1)$$

We write

$$\rho_1 = \frac{1}{2} \nu + \delta, \quad \rho_1 = \frac{1}{2} \nu - \delta, \quad (3.2)$$

where  $\delta=0$  if  $h=0$  in the paramagnetic case. We keep all terms in an expansion in  $\delta$  up to second-order terms. In particular

$$\mathcal{E} \cong \mathcal{E}_0 + \mathcal{E}_1 \delta + \mathcal{E}_2 \delta^2 \quad (3.3)$$

and, if  $\rho_\sigma(S_0)$  and  $\tau_\sigma(S_0)$  are considered functions of the Fermi levels  $S_0$ , we obtain

$$S_0 \cong S_0 \pm \frac{\delta}{\rho'(S_0)} - \frac{1}{2} \frac{\rho''(S_0) \delta^2}{[\rho'(S_0)]^3} \quad (3.4)$$

and

$$\tau_\sigma \cong \tau(S_0) \pm \frac{\tau'(S_0)}{\rho'(S_0)} \delta - \frac{\delta^2}{2Z \rho'(S_0)} \quad (3.5)$$

Complete expressions for  $\mathcal{E}_0$ ,  $\mathcal{E}_1$ , and  $\mathcal{E}_2$  are given in Appendix B. All these are explicit functions of the magnetic field  $h$ . The minimization described in Eq. (2.16) with its attendant constraints is now reduced to a minimization with respect to  $\delta$  in Eq. (3.3). This yields

$$\mathcal{E}_{\text{eq}} = \mathcal{E}_0 - \mathcal{E}_1^2 / 4 \mathcal{E}_2 \quad (3.6)$$

and the susceptibility is given by

$$\chi / \left( \frac{1}{2} g_e \mu_B \right)^2 = [-\mathcal{E}_0'' + (\mathcal{E}_1')^2 / 2 \mathcal{E}_2]_{h=0} \quad (3.7)$$

and the magnetization  $M$  by

$$\frac{M}{\frac{1}{2} g_e \mu_B} = -\mathcal{E}_0' + \frac{\mathcal{E}_1}{4(\mathcal{E}_2)^2} (2\mathcal{E}_2 \mathcal{E}_1' - \mathcal{E}_2' \mathcal{E}_1), \quad (3.8)$$

where all derivatives are with respect to  $h$ . In particular, since  $\mathcal{E}_1$  is odd in  $h$  and  $\mathcal{E}_0$  even in  $h$ ,  $M(h=0) = 0$  as expected for a paramagnetic state.

The susceptibility expression (3.7) consists of two terms. The first term ( $-\mathcal{E}_0''$ ) can be called a Van

Vleck contribution; it arises from magnetic moment of the ionic configuration  $(4f)^{n+1}$  as it is mixed into the ground state by the hybridization. The second term  $[(\mathcal{E}_1')^2 / 2 \mathcal{E}_2]$  is a modified Pauli susceptibility. It reduces exactly to the Pauli form when  $V=0$ , and it contains (as discussed later) a typical Hubbard ferromagnetic enhancement and a modified magnetic-field-dependent bandwidth.

In what follows we show the results of explicit calculations as applied to specific band-structure models.

#### A. Simple cubic band

For a symmetric simple cubic band with nearest-neighbor interactions only  $S_m = -6$  and  $S_M = +6$ . In Table I we give the one-to-one correspondence between  $S_0$  and the number of electrons  $\nu$ . In Fig. 1 we show the susceptibility as a function of  $S_0$  and for  $t/E = -0.02$ ,  $g_0 = 3$ , and various values of the hybridization  $V/E$ . As  $V=0$  we obtain the usual replica of the density of states of the normal Pauli susceptibility. For finite values of  $V$  there is a considerable enhancement and for  $V \sim E$  an enhancement factor of the order of 100 can be observed. As a function of the number of electrons (or equivalently  $S_0$ ) there is a value of  $V/E$  for which the susceptibility diverges; this indicates instability with respect to ferromagnetism. In Fig. 2 we show in the  $(t, V)$  plane

TABLE I: Relationship between  $S_0$  and the number of electrons,  $\nu$ , in the conduction band.

$\nu$	Simple cubic	$S_0$ Face-centered cubic	Rectangular density of states
0	-6	-12	-z
0.2	-3.7	-5.3	-0.8z
0.4	-2.5	-2.7	-0.6z
0.6	-1.6	-1.0	-0.4z
0.8	-0.8	0.1	-0.2z
1.0	0	1.0	0
1.2	0.8	1.6	0.2z
1.4	1.6	2.3	0.4z
1.6	2.5	3.0	0.6z
1.8	3.7	3.6	0.8z
2.0	6	4.0	z

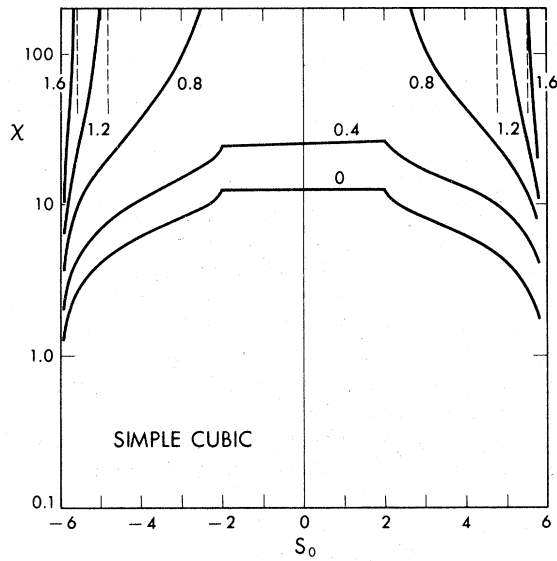


FIG. 1. Susceptibility for a simple cubic example as a function of  $S_0$  for various values of  $V/E$ . The parameters are  $t/E = -0.02$  and the ratio of the ionic to the band  $g$  factors is 3. The one-to-one correspondence between  $S_0$  and the number of electrons is given in Table I. Note the divergence of the susceptibility for given values of the parameters.

the line divergent susceptibility for various values of  $S_0$ . For values of  $V$  larger than those on the curve, the paramagnetic state is unstable. It should be noted that that instability occurs for  $V \sim E$  in all cases.

#### B. Face-centered-cubic band

Similar graphs to those shown in Sec. III A are shown here for a nearest-neighbor only face-centered-cubic band. Here  $S_m = -12$  and  $S_M = 4$  and the band is asymmetric. The correspondence between  $S_0$  and  $\nu$  is given in Table I. Figure 3 shows the susceptibility as a function of  $S_0$  for  $t/E = -0.02$ ,  $g_0 = 3$ , and various values of  $V/E$ . Figure 4 gives the values of  $t/E$  and  $V/E$  for which the susceptibility diverges, with  $S_0$  being a parameter in this case. The results are qualitatively similar to those for the simple cubic example, except that the band density of states is asymmetric and therefore so are the susceptibility and the instability curves.

#### C. Band with a rectangular density of states

Although the theory we developed assumes a known crystal structure with well-defined number and location of the nearest neighbors, the relation (2.10) [see also Appendix A] allows us to extend our

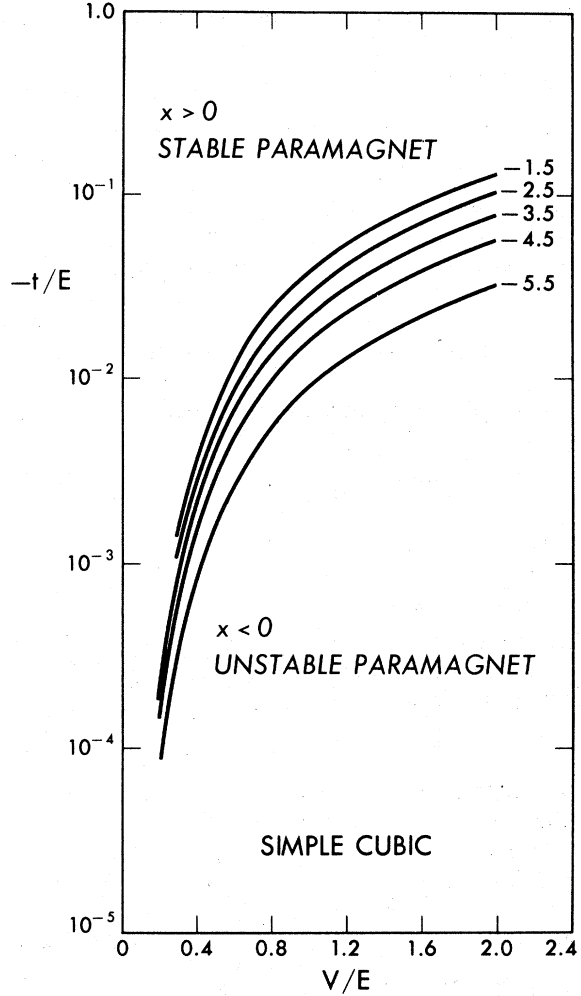


FIG. 2. Curves of diverging susceptibility for the simple cubic case of Fig. 1 in the  $(-t/E)-(V/E)$  plane and for various values of  $S_0$ . Curves for positive values of  $S_0$  are almost identical to the corresponding negative values ( $-S_0$ ).

calculation to an arbitrary density-of-state curve if we specify the number of neighbors  $z$ . In particular for a rectangular density of states, i.e., a constant value between  $S_m$  and  $S_M$  and zero otherwise, all integrals in our calculation can be performed analytically and thus we can shed more light into the physical mechanisms of our model. We choose  $S_m = -z$ ,  $S_M = z$ , and

$$\rho(S) = (S + z)/2z \quad (3.9)$$

and the use of Eq. (2.10) yields

$$\tau(S) = \rho(S) - [\rho(S)]^2 \quad (3.10)$$

With these expressions we obtain from Eq. (3.2)

$$\delta = \frac{1}{2}(\rho_1 - \rho_l) = \frac{1}{2}z(S_1 - S_l) \quad (3.11)$$

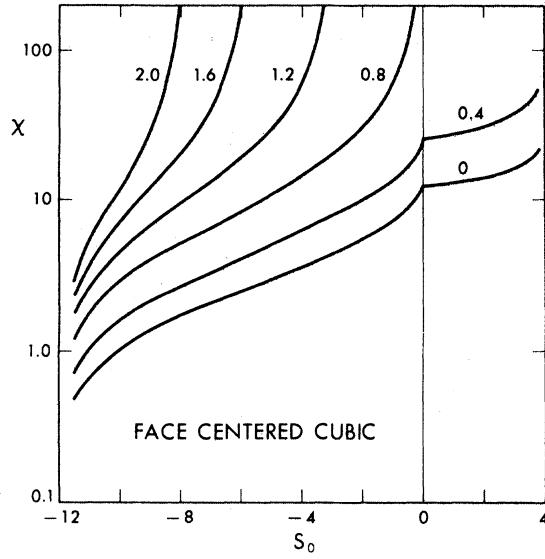


FIG. 3. Susceptibility for a face-centered-cubic example as a function of  $S_0$  for various values of  $V/E$ . The parameters are  $t/E = -0.0$  and the ratio of the ionic to the band  $g$  factors is 3. The one-to-one correspondence between  $S_0$  and the number of electrons is given in Table I. Note the asymmetry of the curves and the divergence of the susceptibility for specific values of the parameters.

The instability condition can be observed by replacing Eqs. (3.9)–(3.11) into the expression of  $\mathcal{E}_2$  in Appendix B, Eq. (B3) and finding values of the parameters which make  $\mathcal{E}_2 = 0$  for  $h = \delta = 0$  [see Eq. (3.7)]. Since in this case  $A_1 = A_1 = A$  and similarly for all other coefficients  $B$  and  $D$ , we obtain

$$2z|t| = \frac{E_{11} - E_1 - E_1}{A + B(2 - \nu) - D(\nu^3/4 - \nu^4/16)} \quad (3.12)$$

If the right-hand side of Eq. (3.12) is smaller than  $2z|t|$ , the paramagnetic state is stable. In Fig. 5 we show the line of instabilities in the  $(t/E)-(V/E)$  plane and in the  $(t/E)-\nu$  plane. The results are again similar to the other two cases, and the instability appears when  $V \sim E$ . Three points are worth remarking. Although the values of the susceptibility depend on the  $g$  factor of the ion and on its magnetic behavior, the curve of instabilities is independent of them. This can be seen from the condition

$$\mathcal{E}_2(h=0) = 0,$$

which determines the instabilities.

A second point of interest is that our fermion Hamiltonian can be reduced to a Hubbard Hamiltonian<sup>3</sup>

$$H_H = \sum_{\langle ij \rangle \sigma} T \gamma_{i\sigma}^\dagger \gamma_{j\sigma} + \sum_i I_0 \nu_{i\uparrow} \nu_{i\downarrow}, \quad (3.13)$$

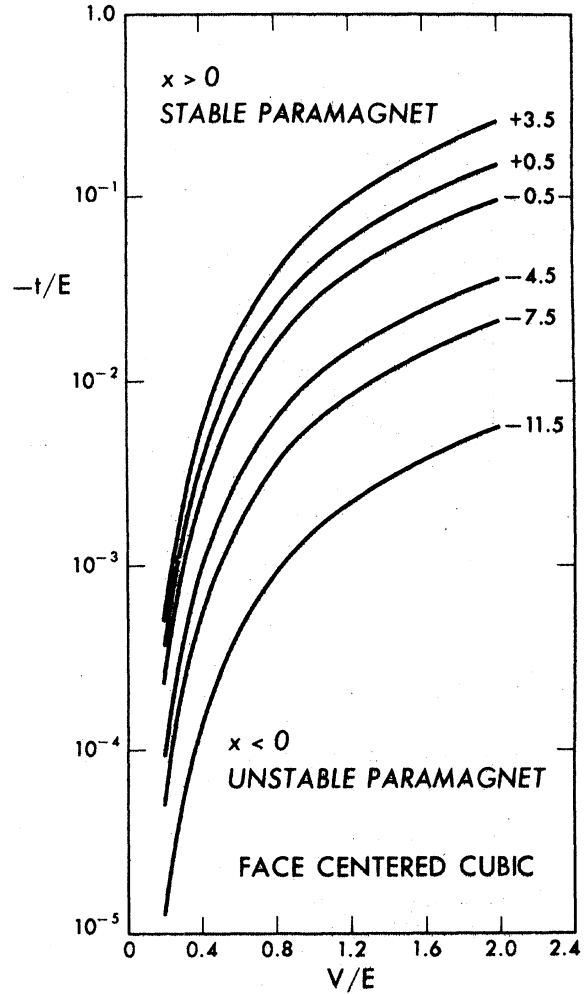


FIG. 4. Curves of divergent susceptibility for the face-centered-cubic case of Fig. 3 in the  $(-t/E)-(V/E)$  plane and for various values of  $S_0$ .

if we make

$$B_\sigma = D_\sigma = 0, \quad tA_\sigma \Rightarrow T, \quad (3.14)$$

$$E_{11} - E_1 - E_1 \Rightarrow I_0.$$

With these changes the ferromagnetic instability condition (3.12) reduces to

$$2z|T| = I_0 \quad (3.15)$$

and, since  $(2z|T|)^{-1} = \mathcal{D}(\epsilon_F)$  is the constant density of states in the rectangular model, this yields the well-known relationship<sup>4</sup>

$$I_0 \mathcal{D}(\epsilon_F) = 1. \quad (3.16)$$

A final point is that although this rectangular

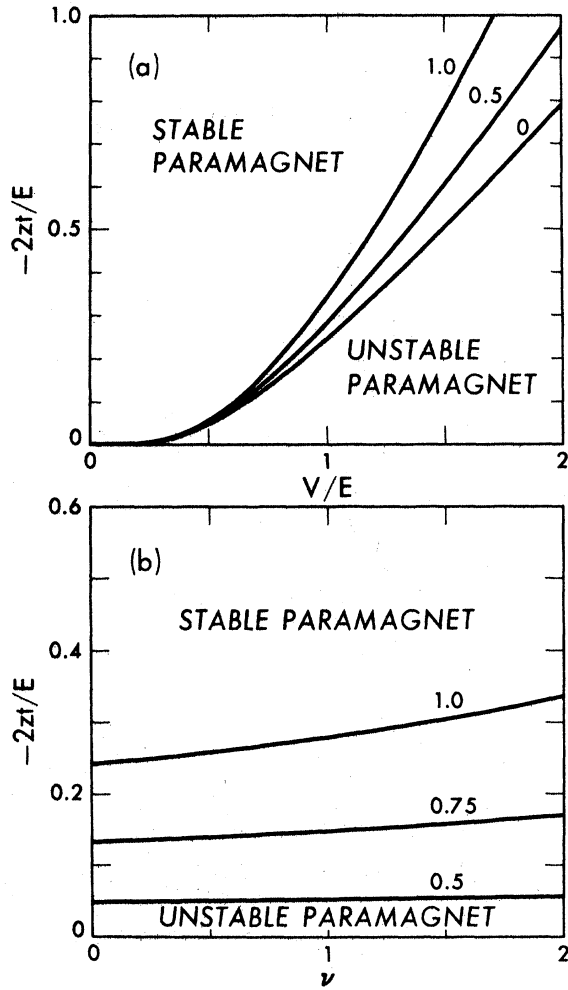


FIG. 5. Curves of divergent susceptibility for the rectangular density-of-state model (a) the  $(t/E)-(V/E)$  plane, with  $\nu$  as a parameter; (b) the  $(t/E)-\nu$  plane, with  $V/E$  as a parameter.

model (and the simple cubic structure as well) is symmetric with respect to electron-hole symmetry, the extra two- and three-particle terms in our Hamiltonian (the  $B_{\uparrow}$ ,  $B_{\downarrow}$ ,  $D_{\uparrow}$ , and  $D_{\downarrow}$  contributions) break this symmetry, albeit only very slightly.

#### IV. ANTIFERROMAGNETIC INSTABILITY

It is known<sup>4</sup> that a Hubbard-type Hamiltonian leads to a large variety of broken symmetry states: antiferromagnetic, ferrimagnetic, and spin-spiral arrangements in addition to the ferromagnetic states. It is thus expected that our Hamiltonian (1.6), which includes several other terms, would produce also a variety of magnetic structures. In this section we re-

strict ourselves to study the instabilities of the paramagnetic state with respect to a single  $\vec{Q}$  antiferromagnetic arrangement, i.e., we study the conditions for a divergent magnetic susceptibility of wave vector  $\vec{Q}$ . We choose  $\vec{Q}$  to be a unique point in the Brillouin zone such that it divides the original crystal structure into two interpenetrating highly symmetric and equivalent sublattices (e.g., two simple cubic structures from a body-centered-cubic lattice, point  $H$  in the bcc Brillouin zone; two face-centered-cubic lattices from a simple cubic crystal,<sup>4</sup> point  $R$  in the sc Brillouin zone). These structures are such that: (i) the density of states is symmetric with respect to electron-hole interchange, and therefore the dimensionless energy parameters  $S(\vec{k})$  such that  $S_m = -S_m$ ; (ii) the relationship

$$S(\vec{k}) = -S(\vec{k} + \vec{Q}), \quad (4.1)$$

is satisfied.

We now define as in Secs. I–III

$$\rho_{i\uparrow} = \frac{1}{2}\nu + \epsilon\eta_i, \quad (4.2)$$

$$\rho_{i\downarrow} = \frac{1}{2}\nu - \epsilon\eta_i,$$

where  $\eta_i = 1$  in one sublattice and  $\eta_i = -1$  in the other. Since not all sites are equivalent, the methods of Secs. II and III are no longer valid. We find

$$U_{i\uparrow} = E_{\uparrow} + (E_{i\uparrow} - E_{\uparrow} - E_{\downarrow})\rho_{i\uparrow} + 2zt(B\tau + D\tau\rho_{i\downarrow}) \quad (4.3)$$

where  $i$  and  $\bar{i}$  are sites in different sublattices, and

$$W_{\uparrow} = -t[A + B\nu + D(\frac{1}{4}\nu^2 - \epsilon^2 - \tau^2) - 2D\tau^2] \quad (4.4)$$

In these equations we have taken  $\hbar = 0$ ,  $A_{\uparrow} = A_{\downarrow} = A$  and similarly for  $B$  and  $D$ , and made explicit the fact that Eq. (2.8b) guarantees that there is only one real  $\tau_{\sigma}$ , labeled  $\tau$ , and it is even in  $\epsilon$ .

We look now at the rectangular density-of-state case of Sec. III C, and look for the instability against antiferromagnetism. This implies that only small values of  $\epsilon$  are relevant. We thus find [see Eq. (3.10)]

$$\tau = \frac{1}{2}\nu - \frac{1}{4}\nu^2 + O(\epsilon^2), \quad (4.5)$$

which yields

$$U_{i\sigma} = U_{\uparrow}(\epsilon=0) \mp [(E_{i\uparrow} - E_{\uparrow} - E_{\downarrow}) + 2ztD\tau]\epsilon\eta_i + O(\epsilon^2) \quad (4.6)$$

and

$$W_{\uparrow} = W_{\uparrow}(\epsilon=0) + O(\epsilon^2). \quad (4.7)$$

In terms of the Bloch operators  $\Gamma_{k\sigma}^{\dagger}$  and  $\Gamma_{k\sigma}$  given in Eq. (2.1), the Hamiltonian is now

$$H_{\text{HF}} = \sum_{k\sigma} E_{k\sigma} \Gamma_{k\sigma}^{\dagger} \Gamma_{k\sigma} + \sum_{k\sigma} \Delta_{\sigma} \Gamma_{k\sigma}^{\dagger} \Gamma_{k+Q\sigma} + K, \quad (4.8)$$

where  $E_{k\sigma}$  and  $K$  have the same meaning as before [see Eqs. (2.2) and (2.3)] and

$$\Delta_\sigma \equiv \mp [(E_{11} - E_1 - E_1) - 2ztD\tau]\epsilon. \quad (4.9)$$

The diagonalization of Eq. (4.8) follows the standard procedure<sup>4</sup> of setting a  $2 \times 2$  secular equation leading to a new canonical transformation

$$\begin{aligned} \Gamma_{1k\sigma} &= u_{k\sigma}\Gamma_{k\sigma} + v_{k\sigma}\Gamma_{k+Q,\sigma}, \\ \Gamma_{2k\sigma} &= -v_{k\sigma}\Gamma_{k\sigma} + u_{k\sigma}\Gamma_{k+Q,\sigma}. \end{aligned} \quad (4.10)$$

From these new one-particle eigenvalues are obtained and a self-consistency equation follows:

$$\begin{aligned} \epsilon &= \frac{1}{2} N^{-1} \sum_i (\rho_{i1} - \rho_{i2}) \eta_i \\ &= N^{-1} \sum_{k\sigma} |u_{k\sigma} v_{k\sigma}| (\langle \Gamma_{1k\sigma}^\dagger \Gamma_{1k\sigma} \rangle - \langle \Gamma_{2k\sigma}^\dagger \Gamma_{2k\sigma} \rangle), \end{aligned} \quad (4.11)$$

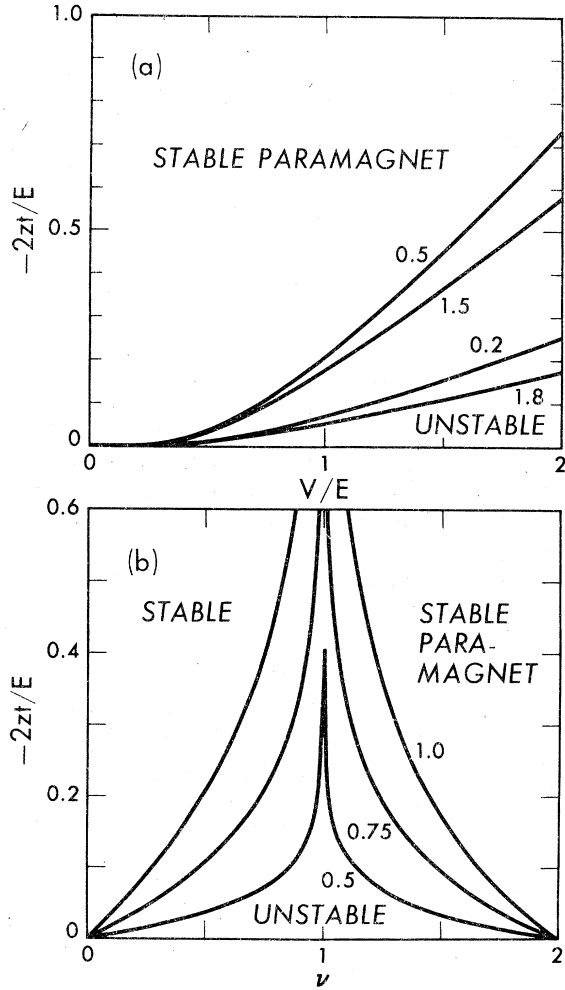


FIG. 6. Curves of antiferromagnetic instability for the rectangular density-of-state model. (a) The  $(t/E)-(V/E)$  plane, with  $\nu$  as a parameter. (b) The  $(t/E)-\nu$  plane with  $V/E$  as parameter.

where  $u_{k\sigma}$  and  $v_{k\sigma}$  are functions of  $\epsilon$ . Since  $\epsilon=0$  is always a solution (the paramagnetic one), the instability condition is obtained by requiring the coefficients of the linear term in  $\epsilon$  on the right-hand side to equal 1, the left-hand side coefficient.

This procedure yields

$$2z|t| = \frac{-(E_{11} - E_1 - E_1)\ln|1-\nu|}{A + B\nu + \frac{1}{4}D\nu^2 - 3D\tau^2 - D\tau\ln|1-\nu|}. \quad (4.12)$$

Figure 6 shows the lines in the  $(t/E)-(V/E)$  plane (with  $\nu$  as a parameter) and in the  $(t/E)-\nu$  plane (with  $V/E$  as a parameter) where Eq. (4.12) is satisfied. Several points are worth remarking:

(i) If the right-hand side of Eq. (4.12) is smaller than  $2z|t|$ , the paramagnetic state is stable. This corresponds to the upper regions of both graphs in Fig. 6.

(ii) If we go once again to the Hubbard limit (3.14) and (3.15), Eq. (4.12) reduces to

$$2z|T| = -I_0 \ln|1-\nu|, \quad (4.13)$$

or, equivalently

$$1 = -I_0 \mathcal{D}(\epsilon_F) \ln|1-\nu|. \quad (4.14)$$

For this particular case and  $\nu=1$  the paramagnetic state is always unstable,<sup>4</sup> which is the usual Peierls instability of these simple models. In our case  $\nu=1$  does not correspond to an always unstable paramagnet. For  $\nu \rightarrow 1$ , we obtain instead of Eq. (4.12),

$$\tau = \frac{1}{4}, \quad z|t| = 2(E_{11} - E_1 - E_1)/D. \quad (4.15)$$

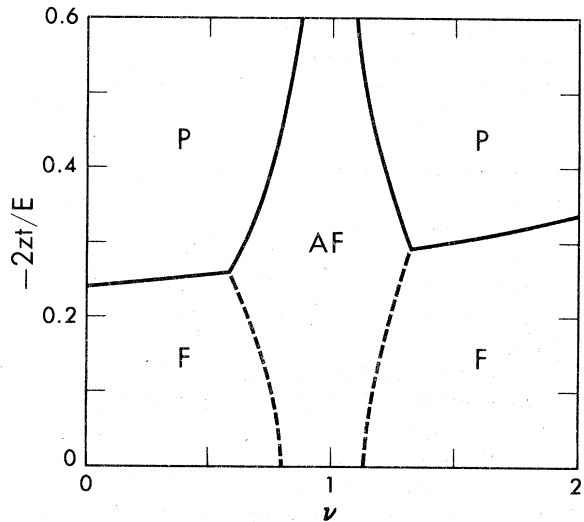


FIG. 7. Schematic phase diagram in the  $t/E-\nu$  plane,  $V/E=1$ . P: paramagnetic state; F: ferromagnetic state; AF: antiferromagnetic state. The boundaries F-AF are estimations only, based on the equivalent Hubbard model.

If, once again,

$$z|t| > 2(E_{11} - E_1 - E_1)/D, \quad (4.16)$$

the paramagnetic state may be stable.

(iii) There is a notable lack of symmetry between electrons and holes. The paramagnetic state is more stable against antiferromagnetism for  $\nu > 1$  than for  $\nu < 1$ . This is opposite to what is found for ferromagnetic instabilities.

(iv) In Fig. 7 we show a schematic phase diagram for  $V = E$ , where the electron-hole asymmetry is evident.

## V. SUMMARY AND CONCLUSIONS

The formalism developed in I to treat intermediate valence solids has been applied to study a variety of magnetic problems. In particular we find:

(i) The normal (paramagnetic) state has a considerably enhanced magnetic susceptibility. It can be considered the addition of two terms: a *ferromagnetically enhanced Pauli susceptibility* similar to that found in Hubbard's model, and a Van Vleck-type contribution caused by the admixture of the excited configuration.

(ii) For values of the hybridization parameter of the order of the energy separation between configurations, the susceptibility tends to diverge, signaling the onset of a ferromagnetic instability. That instability is more apparent for cases in which the density of states at the Fermi level is larger.

(iii) The Van Vleck-type susceptibility appears only when the excited configuration is a multiplet, and requires different magnetic moments for the band electrons and the excited ion.

(iv) The ferromagnetic instability is independent of the Van Vleck-type contribution to the susceptibility.

(v) Other types of instabilities are also possible. Of these we have only examined a specific example of the antiferromagnetic case, corresponding to bands which yield perfect nesting of the Fermi surface in the half-filled band situation. As expected, in this particular situation the antiferromagnetic instability tends to dominate, but it is not present in the limiting case of vanishing hybridization, in contraposition to the ordinary Hubbard Hamiltonian.<sup>4</sup>

Two points should be emphasized: (a) The enhanced susceptibility in paramagnetic configurations is the most striking feature of the magnetic properties of all mixed-valent solids<sup>5</sup>; our theory shows this effect. (b) Since we have used a Hartree-Fock-type factorization, our results will show the quantitative overestimation inherent in such approximation<sup>6</sup>; this should be kept in mind when comparing numerical values to actual experimental data.

Study of other properties, e.g., specific heat and lattice dynamics would be of considerable interest to compare our model with the experimentally well-studied intermediate-valence solids.

## ACKNOWLEDGMENTS

This work was supported by the U. S. National Science Foundation through Grants No. DMR78-03408 and No. INT76-05452 and by the Brazilian CNPq through the Cooperative Science Program UNICAMP-UC Berkeley. One of us (M. E. F.) is grateful to the staff of the Department of Physics, UC Berkeley for their hospitality during part of this work. Another of us (C. A. B.) was supported in part by the Consejo Nacional de Investigaciones Cientificas y Tecnicas (CNICT), Argentina.

## APPENDIX A

Since the definition (2.7) does not depend on the particular nearest-neighbor  $\delta$  chosen, we can sum over all  $\delta$  and divide by the number  $z$  of nearest neighbors, i.e.,

$$\tau(S_\sigma) = (zN)^{-1} \sum_{\delta} \sum_k \exp(i\vec{k} \cdot \vec{R}_\sigma) f_\sigma(\vec{k}) \quad (A1)$$

(with  $nn$  being nearest neighbors) which, by means of Eq. (2.4) reduces to

$$z\tau(S_\sigma) = -(N)^{-1} \sum_k S(\vec{k}) f_\sigma(\vec{k}) \quad (A2)$$

Since, according to Eq. (2.5),  $f(\vec{k})$  is also a function of  $S(\vec{k})$  only, a change of variable from  $\vec{k}$  to  $S(\vec{k})$  and the use of Eq. (2.6) yields Eq. (2.10). This can also be written in the form

$$z \frac{d\tau_\sigma}{dS_\sigma} = -S_\sigma \frac{d\rho_\sigma}{dS_\sigma} \quad (A3)$$

## APPENDIX B

The coefficients for the energy expansion (3.3) are

$$\begin{aligned} \mathcal{E}_0 &= (E_1 + E_1)\rho_0 + (E_{11} - E_1 - E_1)\rho_0^2 \\ &+ zt[(A_1 + A_1)a_0 + 2(B_1 + B_1)b_0 \\ &+ (D_1 + D_1)d_0] \quad (B1) \end{aligned}$$

$$\begin{aligned} \mathcal{E}_1 &= (E_1 - E_1) + zt[(A_1 - A_1)a_1 + 2(B_1 - B_1)b_1 \\ &+ (D_1 - D_1)d_1] \quad (B2) \end{aligned}$$

$$\begin{aligned} \mathcal{E}_2 &= -(E_{11} - E_1 - E_1) \\ &+ zt[(A_1 + A_1)a_2 + 2(B_1 + B_1)b_2 \\ &+ (D_1 + D_1)d_2] \quad (B3) \end{aligned}$$



where

$$\tau_1 \cong a_0 + a_1\delta + a_2\delta^2 + \dots, \quad (\text{B4})$$

$$\rho_1\tau_1 \cong b_0 + b_1\delta + b_2\delta^2 + \dots, \quad (\text{B5})$$

$$(\rho_1^2 - \tau_1^2)\tau_1 \cong d_0 + d_1\delta + d_2\delta^2 + \dots, \quad (\text{B6})$$

and the expansions (B4)–(B6) are obtained by means of Eqs. (3.2) and (3.5).

\*On leave from Centro Atomico Bariloche, Argentina.

<sup>1</sup>M. E. Foglio and L. M. Falicov, Phys. Rev. B 20, 4554 (1979) (preceding paper).

<sup>2</sup>M. E. Foglio, J. Phys. C 11, 4171 (1978).

<sup>3</sup>J. Hubbard, Proc. R. Soc. London Sect. A 277, 237 (1964); 281, 401 (1964).

<sup>4</sup>D. R. Penn, Phys. Rev. 142, 350 (1966).

<sup>5</sup>*Valence Instabilities and Related Narrow-Band Phenomena*, edited by R. D. Parks (Plenum, New York, 1977).

<sup>6</sup>See for instance, C. Herring, in *Exchange Interactions among Itinerant Electrons*, edited by G. T. Rado and H. Suhl (Academic, New York, 1966), Vol. IV of *Magnetism*.